

Shape Determination of Elastica Subjected to Bending by Means of Displacements

DOI: 10.5604/12303666.1221748

Department of Technical Mechanics
and Computer Science,
Lodz University of Technology,
ul. Zeromskiego 116, 90-924 Lodz, Poland
E-mail: piotr.szablewski@p.lodz.pl

Abstract

Free folding of flat textiles can be determined using elastica for the same shape, loads and folding conditions across the product. The paper presents a general theory concerning shape determination of coplanar elastica subjected to static bending by means of displacements. The displacements are described by the coordinates of points of initially unbending elastica and the loads imposed. The physical behavior of elastica is described using some simplifications by both physical and mathematical models. The mathematical model can be discussed using a solution of six nonlinear differential equations with appropriate boundary conditions. Three relationships are the equations of equilibrium, and the other describes the displacements along the particular axis, the change in curvature and the physical law.

Key words: bending; elastica; displacement method; numerical analysis; shooting method; large deflections.

Introduction

Textiles usually have the same cross-section as well as repeatable loads and folding conditions across the product. Thus the free folding of flat textile products can be determined using elastica i.e. within its optimal cross-section. The problem is complicated and the flat deflection curve described as heavy elastica is formulated under the decisive influence of the force of gravity.

The application of fibres in different structures and as reinforcement in composite materials requires, in most cases, quantitative analysis of their mechanical properties. The adoption of perfect fibres made of a homogeneous material of constant circular cross-section leads to an analysis of the bending, analogous to the analysis of bending concerning the homogeneous elastica. Because of elastica properties, methods of analysis resulting from the classical theory of the strength of materials are useless. Even the classical linear theory of elasticity, because of the adoption of small displacements and deformations, is not suitable during the analysis in respect of large deformations. Most of the works concerning the bending of elastica are based on the Bernoulli-Euler law.

$$\frac{1}{\rho^*} - \frac{1}{\rho} = \frac{M}{EI}, \quad (1)$$

where, ρ^* is the radius of curvature of elastica subjected to bending, ρ the radius of curvature of the initially unbending curve, M the bending moment in the cross-section of elastica, and EI is the bending stiffness.

Several papers published in recent years concern the large deflection of thin rods using the Bernoulli-Euler law. Most of them are described in [1], including some numerical methods to solve the problems selected. General equations are considered by Scott, Carver, and Kan [2] using the method of return to the original state, which leads to solutions in the form of a non-linear equation in a rectangular coordinate system in the case of vertical forces. Assuming the solutions as functions expanded in an infinite series, the nonlinear equations are reduced to a system of linear equations, which can be solved by integration. Some numerical examples are also included.

Chicurel and Suppiger [3] have recently applied the energy methods to find the large deflection of statically loaded textile fibres. For circular fibres acting as a cantilever with a horizontal force and moment applied to the free end, the solutions were determined in terms of elliptic integrals. Several other problems were solved numerically using a digital computer. The problem of large deflection can be solved by means of both physical and mathematical models of the planar bending curve and elastica (Love [4], Szablewski [5, 6], Bickley [7], FrischFay [1]). Interesting information about elastica was published by Levien [8]. This report traces the history of elastica from its first precise formulation by James Bernoulli in 1691 through to the present. A mathematical model of elastica and solution methods of differential equations are presented, for example, by Szablewski [9], including a shooting method for numerical analysis of Peirce's cantilever test. Moreover the application of numeri-

cal methods in respect of specific problems existing in textile engineering was also discussed. More recent investigations of elastica and nonlinear problems can be found in [10 - 14].

References [15, 16] provide a number of results for the tensile deformation of fibres with planar waviness (crimp). Semi-circular arcs connected with sinusoidal shapes subjected to small loads were analyzed. Large deformation problems of filaments were also applied to study the deformation behavior of collagen fibres in connective tissue [17 - 19]. Some problems concerning the behavior of fibres subjected to different loads are discussed in [20 - 23].

The work presented applies to statically loaded elastica subjected to bending. The main goal is to determine the shape of the deflected curve as a function of the original undeformed shape and loads imposed. The solution depends on the normal and tangential displacement of points located on the initially undeformed curve. The novelty elements are the presented advanced description of elastica deflections using the non-linear differential equations as well as the sensitivity analysis of the dependences obtained in respect of some selected parameters.

In this paper some assumptions are introduced to simplify the problem.

- i) The elastica axis is coplanar.
- ii) The material is homogeneous, isotropic and subject to Hooke's law.
- iii) The cross-section of elastica is circular, of constant diameter, and small in comparison with the radius of curvature and the length of the axis.

- iv) The cross-sections of elastica are always planes.
- v) The normal stresses perpendicular to the axis of elastica are negligible.
- vi) Elastica is inextensible. Mathematically speaking, the result of the analysis is a system of six nonlinear differential equations describing elastica subjected to bending.

Modeling and methods

Analysis of displacements

Let us introduce two infinitesimal elements of statically loaded elastica of the coplanar axis: ds in the initial state (i.e. undeformed shape) and ds^* in the deformed shape subjected to bending, cf. **Figure 1**. The symbols without stars refer to the undeformed curve, whereas the symbols marked with an asterisk (*) apply to the deflected curve.

Let us first determine the relationship between the tangent strains and displacements. The location of an optional point P on the elastica curve is described by the tracing vector \bar{r} , cf. **Figure 2**.

We can denote according to **Figure 2** the measure of vector $|\bar{r}| = r$. Introducing the geometrical correlations, the following equation can be derived:

$$\frac{d\bar{r}}{ds} = \bar{t}, \quad (2)$$

where, \bar{t} is the unit vector tangent to undeformed elastica of the positive sense compatible with the growth direction of arc variable s . From **Equation 2** we obtain:

$$\begin{aligned} d\bar{r} &= ds \cdot \bar{t}, \\ |d\bar{r}| &= ds. \end{aligned} \quad (3)$$

Let us determine the displacement of an optional point $P \rightarrow P^*$ described by vectors \bar{r} and \bar{r}^* , respectively. Thus the following symbols are now introduced: v – normal displacement, u – tangent displacement, ε – relative strain.

The variable position of point P is determined by vector \bar{r}^* in the form (**Figure 3**):

$$\bar{r}^* = \bar{r} + \bar{w} = \bar{r} + u \cdot \bar{t} + v \cdot \bar{n}, \quad (4)$$

where, \bar{n} is the unit vector directed from the center point of curvature along

the normal to the curve directed outwards. Derivative $\frac{d\bar{r}^*}{ds}$ is in fact the infinitesimal increment of vector \bar{r}^* in respect of arc variable s and can be expressed by equation:

$$\frac{d\bar{r}^*}{ds} = \frac{d\bar{r}}{ds} + \frac{du}{ds} \cdot \bar{t} + u \cdot \frac{d\bar{t}}{ds} + \frac{dv}{ds} \cdot \bar{n} + v \cdot \frac{d\bar{n}}{ds} \quad (5)$$

The Frenet equations [24] for the plane curve are as follows:

$$\begin{aligned} \frac{d\bar{t}}{ds} &= -\kappa \cdot \bar{n} = -\frac{\bar{n}}{\rho}, \\ \frac{d\bar{n}}{ds} &= \kappa \cdot \bar{t} = \frac{\bar{t}}{\rho}. \end{aligned} \quad (6)$$

where, κ is the curvature. Because $\frac{d\bar{r}^*}{ds} = \frac{ds}{ds^*} \frac{d\bar{r}^*}{ds^*}$ then introducing **Equation 6** into **Equation 5** and separating the variables, we obtain the equivalent formulation.

$$d\bar{r}^* = ds \left[\left(1 + \frac{du}{ds} + \frac{v}{\rho} \right) \cdot \bar{t} + \left(\frac{dv}{ds} - \frac{u}{\rho} \right) \cdot \bar{n} \right], \quad (7)$$

The measure of vector $d\bar{r}^*$ can be consequently described as follows:

using $\frac{d\bar{r}^*}{ds^*} = \bar{t}^*$ and $|\bar{t}^*| = 1$ we have **Equation 8**.

$$\begin{aligned} |d\bar{r}^*| &= ds^* = \\ &= ds \left[\left(1 + \frac{du}{ds} + \frac{v}{\rho} \right)^2 + \left(\frac{dv}{ds} - \frac{u}{\rho} \right)^2 \right]^{\frac{1}{2}} \end{aligned} \quad (8)$$

The relative strain can be defined in accordance with the definition:

$$\varepsilon = \frac{ds^* - ds}{ds} = \frac{ds^*}{ds} - 1. \quad (9)$$

Equation 8 can be included in **Equation 9**, which allows to determine the relative strain:

$$\varepsilon = \left[\left(1 + \frac{du}{ds} + \frac{v}{\rho} \right)^2 + \left(\frac{dv}{ds} - \frac{u}{\rho} \right)^2 \right]^{\frac{1}{2}} - 1 \quad (10)$$

The elastica is inextensible, i.e. $\varepsilon = 0$ and $\frac{ds^*}{ds} = 1$, which allows to formulate.

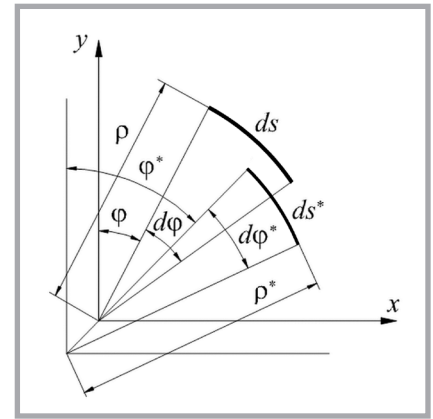


Figure 1. Infinitesimal elements ds of undeformed and ds^* of deformed elastica.

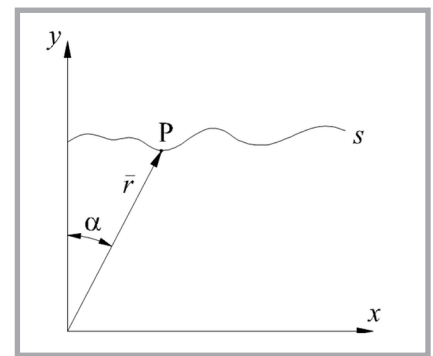


Figure 2. Undeformed plane curve with point P determined by tracing vector \bar{r} .

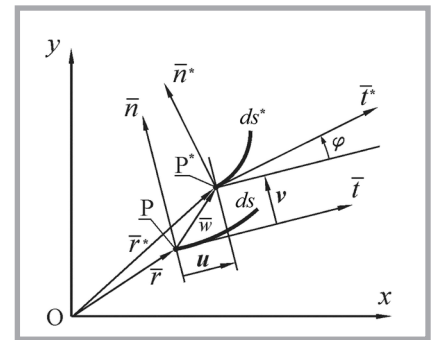


Figure 3. Part of undeformed and deformed elastica with displacements of point P.

$$\left[\left(1 + \frac{du}{ds} + \frac{v}{\rho} \right)^2 + \left(\frac{dv}{ds} - \frac{u}{\rho} \right)^2 \right]^{\frac{1}{2}} - 1 = 0 \quad (11)$$

Equation 11 takes the form after reduction:

$$\begin{aligned} &\left(\frac{du}{ds} + \frac{v}{\rho} \right) + \\ &+ \frac{1}{2} \left[\left(\frac{du}{ds} + \frac{v}{\rho} \right)^2 + \left(\frac{dv}{ds} - \frac{u}{\rho} \right)^2 \right] = 0 \end{aligned} \quad (12)$$

This is a condition of inextensibility, expressed by means of the displacements.

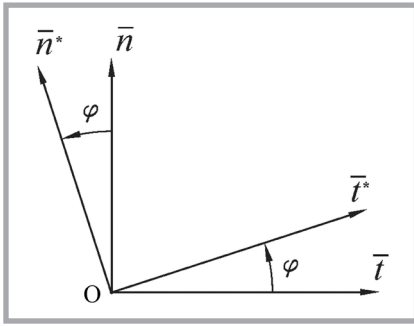


Figure 4. Normal and tangential vectors translated to act through vertex O .

The relationship between the curvature of the deformed elastica and displacements will be next derived. From Equation 6 it is known that $\frac{d\bar{t}}{ds} = \frac{\bar{n}}{\rho}$, but $\frac{d\bar{r}}{ds} = \bar{t}$, and then $\frac{d\bar{t}}{ds} = \frac{d^2\bar{r}}{ds^2}$. Finally it can be denoted:

$$\frac{d^2\bar{r}^*}{ds^{*2}} = \frac{\bar{n}^*}{\rho^*}. \quad (13)$$

The corresponding measure has the form

$$\left| \frac{d^2\bar{r}^*}{ds^{*2}} \right| = \frac{1}{\rho^*}. \quad (14)$$

Due to the condition of inextensibility $ds = ds^*$, Equation 14 can be rewritten as follows:

$$\left| \frac{d^2\bar{r}^*}{ds^2} \right| = \frac{1}{\rho^*}. \quad (15)$$

Let us next determine the second-order derivative $\frac{d^2\bar{r}^*}{ds^2}$ by means of Frenet Equations 6 and relationships $\frac{d^2\bar{t}}{ds^2} = -\frac{\bar{t}}{\rho^2}$ and $\frac{d^2\bar{n}}{ds^2} = -\frac{\bar{n}}{\rho^2}$. The reduction of the above equation allows to describe.

$$\frac{d^2\bar{r}^*}{ds^2} = \left[\frac{d^2u}{ds^2} + \frac{2}{\rho} \frac{dv}{ds} - \frac{u}{\rho^2} \right] \cdot \bar{t} + \left[-\frac{d^2v}{ds^2} + \frac{2}{\rho} \frac{du}{ds} + \frac{1}{\rho} + \frac{v}{\rho^2} \right] \cdot \bar{n} \quad (16)$$

assuming that the initial curvature $\kappa = 1/\rho$ is constant.

We have to consider the Bernoulli-Euler law (1) and Equation 15, noting the equation

$$\left(\frac{d^2\bar{r}^*}{ds^2} \right)^2 = \left(\frac{1}{\rho^*} \right)^2 = \left(\frac{M^*}{EI} + \frac{1}{\rho} \right)^2 \quad (17)$$

Introducing once again the Bernoulli-Euler law into Equation 16, we obtain immediately:

$$\left(\frac{M^*}{EI} + \frac{1}{\rho} \right)^2 = \left[\frac{d^2u}{ds^2} - \frac{2}{\rho} \frac{dv}{ds} - \frac{u}{\rho^2} \right]^2 + \left[-\frac{d^2v}{ds^2} + \frac{2}{\rho} \frac{du}{ds} + \frac{1}{\rho} + \frac{v}{\rho^2} \right]^2. \quad (18)$$

In order to find an expression for the rotation angle in terms of displacements, we must consider the following dot products:

$$\begin{aligned} \bar{t} \cdot \bar{t}^* &, \\ \bar{n} \cdot \bar{t}^* &. \end{aligned} \quad (19)$$

From the Figure 4 we have

$$\begin{aligned} \bar{t} \cdot \bar{t}^* &= |\bar{t}| \cdot |\bar{t}^*| \cos(\varphi), \\ \bar{n} \cdot \bar{t}^* &= |\bar{n}| \cdot |\bar{t}^*| \cos\left(\frac{\pi}{2} - \varphi\right). \end{aligned} \quad (20)$$

Since \bar{t} , \bar{t}^* , and \bar{n} are all unit vectors

$$\begin{aligned} \bar{t} \cdot \bar{t}^* &= \cos(\varphi), \\ \bar{n} \cdot \bar{t}^* &= \sin(\varphi). \end{aligned} \quad (21)$$

Because $\frac{d\bar{r}^*}{ds^*} = \bar{t}^*$ and $ds^* = ds$ (condition of inextensibility), then from Equation 7 and Figure 4 we have the vector quantity \bar{t}^* .

$$\begin{aligned} \cos \varphi &= 1 + \frac{du}{ds} - \frac{v}{\rho}, \\ \sin \varphi &= \frac{dv}{ds} + \frac{u}{\rho}. \end{aligned} \quad (22)$$

The rotation angle φ is now defined by Equation 22.

Equations of equilibrium

The problem can be additionally supplemented by equilibrium conditions. Thus we consider an elastica element of length ds , whereas the loads are applied according to Figure 5.

The internal forces within the cross-section of elastica are reduced to the horizontal force F_x , vertical force F_y , as well as the bending moment M . The external forces (i.e. the loading forces) are the continuous load q and tangential load p . However, the continuous load q does not always exist within the real elastica. This load can be characterized by the fixed direction of action i.e. the constant angle. Thus the angle does

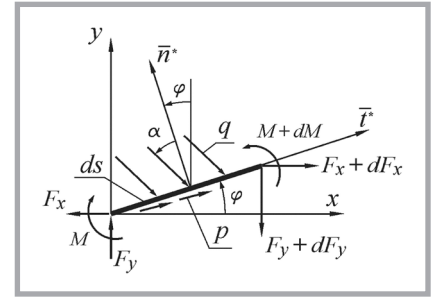


Figure 5. Elementary sector of deformed elastica with imposed loads.

not change with the variation of the angle of inclination between the horizontal and tangential to the elastica at any point of the curve. Alternatively the load can work in the tracing direction, that is, the direction changes when the tangent to the elastica changes. The second case is shown in Figure 5.

According to the figure, the direction of continuous load is determined by the constant angle measured to the normal direction \bar{n} . Moreover the angle of inclination between the vertical axis y and the normal direction \bar{n} is equal to. Of course, the normal direction varies along the elastica with a change in any point on the curve specified by the arc variable s . Therefore the tracing continuous load q has a variable direction along the deformed curve. It is characterized by a constant angle in respect of the normal \bar{n} . In the case of a fixed continuous load, its deviation from the normal direction is not considered.

In this case, the angle represents the deviation from the vertical direction. An example of this load can be the gravitational field i.e. the downwardly directed linear weight of the angle $= 0$. The balance of an infinitesimal elastica element (Figure 5) allows to formulate the balance equations.

$$\frac{dF_x}{ds} = -q \cdot \sin(\varphi + \alpha) - p \cdot \cos \varphi, \quad (23)$$

$$\frac{dF_y}{ds} = -q \cdot \cos(\varphi + \alpha) + p \cdot \sin \varphi, \quad (24)$$

$$\frac{dM}{ds} = F_x \sin \varphi + F_y \cos \varphi. \quad (25)$$

An optional problem concerning elastica of large deflection of initial curvature $\kappa = 1/\rho$ is determined by Equations 23 & 25 (i.e. equations of equilibrium) accompanied by Equations 12, 18 and 22 (i.e. equations connecting the displacements and conditions of equilibrium) as well as the Bernoulli-Euler law - Equa-

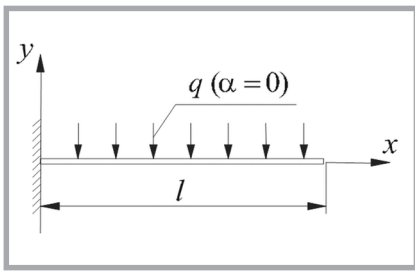


Figure 6. Rectilinear horizontal elastica fixed at one end and unbounded at the other.

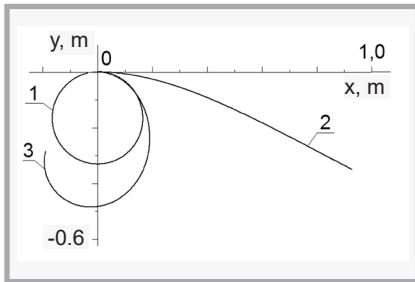


Figure 7. Deflection of elastica under various loads: 1) bending moment $M = 0.004 \text{ Nm}$ at the free end, 2) continuous load $q = 0.002 \text{ N/m}$ ($\alpha = 0$), 3) simultaneously applied bending moment $M = 0.004 \text{ Nm}$ and continuous load $q = 0.014 \text{ N/m}$ ($\alpha = 0$).

tion 1. All these equations allow for the solution of any large deflection problem involving fibres. In the case of a continuous load with a constant direction of action, *Equations 23* and *24* should contain the angle of inclination = 0 in trigonometric functions. Additionally these equations should be supplemented by appropriate boundary conditions, usually associated with the ends of elastica (but not only).

The unknowns are F_x , F_y , M , φ , u , v . Generally not all values of unknowns are determined at the starting point of the integration interval. Therefore *t* appropriate methods to solve the boundary problem presents should be applied (e.g. shooting method). Let us introduce asimple example of elastica (*Figure 6*) which is fixed at one end and unbounded at the other. The shape is rectilinear horizontal and loaded with only a continuous constant load. Thus the initial curvature $1/\rho = 0$, $ds = dx$ whereas the boundary conditions are the following.

$$\begin{aligned} \text{for } x = 0, u = v = \varphi = 0, \\ \text{for } x = l, F_x = F_y + M = 0. \end{aligned} \quad (26)$$

However, these equations are complicated enough for the general case. The difficulty can be minimized by means of numerical calculations to solve most

of the problems related to this matter. Consider the case of elastica restrained at one end and subjected to pure bending by the bending moment M at the free end. The solutions of *Equations 23, 25, 12, 18, 1* can be obtained in finite form for the displacements specified. These have the form.

$$u = \frac{1}{k} \sin kx - x, \quad v = \frac{1}{k} (\cos kx - 1), \quad (27)$$

$$\text{where, } k = \frac{M}{E}.$$

Results and discussion

Numerical examples

The set of equations is solved for elastica of the initial rectilinear shape, restrained at one end, and for the following parameters: Young's modulus $E = 2.1 \times 10^5 \text{ MPa}$, cross-sectional diameter $d = 5 \times 10^{-4} \text{ m}$, and length $l = 1 \text{ m}$. The solution of this boundary value problem was based on the shooting method. The results are graphically presented in *Figures 7* and *8* for the various types of loads selected.

Figure 7 shows solutions for the following cases: (1) the bending moment M applied at the free end, (2) the continuous load q applied downward along the entire length of elastica, (3) both the bending moment M and continuous load q simultaneously applied. It is easily seen that the adequate bending moment causes a circular form of the deformed elastica, that is, the shape of the optimal bending rigidity. The second problem generates the typical shape of a curve subjected to a continuous vertical load, which is well known for the strength of materials. The loads simultaneously applied give a helix elastica of average shape between the circle and classical bending line of the beam.

All shapes in *Figure 8* have the form of a helix. Decisive is the sign of the inclination angle α of continuous load q . The positive values indicate the load acting downwards, while the negative – operating upwards. The larger the inclination angle, the greater the horizontal component of the load. Thus the vertical component is getting smaller.

The greater the positive value of the inclination angle, the smaller the local radius of helix curvature. The reason is the growing influence of the bending moment, whereas the impact of the con-

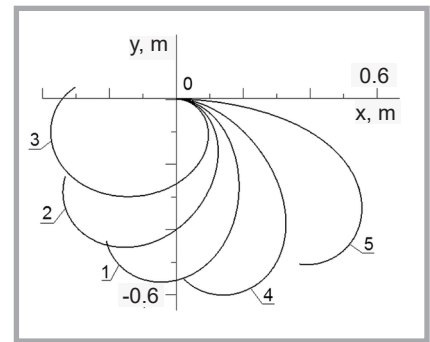


Figure 8. Elastica obtained for simultaneously applied bending moment $M = 0.004 \text{ Nm}$ and continuous load $q = 0.02 \text{ N/m}$ for different inclination angles α : 1) $\alpha = 0$, 2) $\alpha = 35^\circ$, 3) $\alpha = 80^\circ$, 4) $\alpha = 35^\circ$, 5) $\alpha = 80^\circ$.

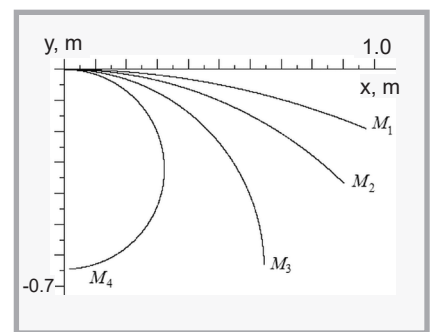


Figure 9. Shapes of deflected elastica subjected to pure bending for different values of bending moment M : $M_1 = 0,25 \cdot 10^3 \text{ Nm}$, $M_2 = 0,50 \cdot 10^3 \text{ Nm}$, $M_3 = 1,0 \cdot 10^3 \text{ Nm}$, $M_4 = 2,0 \cdot 10^3 \text{ Nm}$.

tinuous load increasingly decreases. On the contrary, the greater the negative value of the angle, the greater the local radius of the helix. Thus the corresponding line is obtained due to the increasing load, which operates upwards.

The shapes of deflected elastica subjected to pure bending are shown in *Figure 9* for several values of the bending moment M .

It is evident in *Figure 9* that the greater the bending moment, the smaller the local radius of curvature of the elastica. The maximal bending moment creates a semicircular shape of elastica i.e. the shape of the convenient bending rigidity.

Conclusions

The problem presented is a model of some real practical applications which can be found in different approaches of textile engineering. Thus textiles after different finishing procedures need the maximal possible path to ensure

the correct technology in a relatively limited time, see, for example, printing, drying etc. The complex 3D problem can be reduced to elastica of different deflections as well as parameters because the boundary values are also variable.

Additionally complex textile composites can be subjected to different loads, which is described by means of changeable deflection curves of the textile structure. Although the analysis is accurate, the equations obtained are relatively uncomplicated and can be solved using a set of standard methods. The problem is easy enough to model, describe, analyze and visualize.

The majority of analysis methods concerning the large deflections of elastica introduce the displacements indirectly. Additionally most of these methods require knowledge of the expression describing the distribution of the bending moment along the entire length of elastica.

The application of normal and tangential displacements of the element during the analysis allows to determine the deflected shape of elastica without knowledge of the bending moment distribution. However, the equations obtained are rather complicated. Some theoretical methods allow to formulate solutions in the form of elliptic integrals.

Therefore the problem can be solved numerically. The shooting method applied to solve the boundary problem is an effective, fast and fairly stable tool to generate the shapes of elastica subjected to bending. The shapes obtained are logical and consistent with those by elementary calculations.

It should be noted that the assumption of inextensible elastica is somewhat limited. However, this is often introduced during analysis of large deflections. Irrespective of the above limitation, we can solve a number of problems related to the bending of elastica assuming its inextensibility. Sometimes it is the only possible solution. An interesting question is also the repeatable geometry, loads and folding conditions across the material. The problem is really complicated and probability mathematics can be intro-

duced to approximate the current boundary conditions.

This kind of problems can be solved by means of various numerical methods. Some solutions may also introduce theory and optimization techniques to determine the optimal shape and/or internal energy of fibres subjected to large deformations. This problem seems to be an interesting continuation of this article to develop in the future.



References

1. Frisch-Fay R. *Flexible Bars*. Butterworth: London, 1962.
2. Scott EJ, Carver DR, Kan M. On the Linear Differential Equation for Beam Deflection. *Journal of Applied Mechanics* 1955; 22: 245-248.
3. Chicurel R, Suppiger E. Load-Deflection Analysis of Fibers with Plane Crimp. *Textile Research Journal* 1960; 30: 568-575.
4. Love AEH. *The Mathematical Theory of Elasticity*. Cambridge University Press: London, 1920.
5. Szablewski P. Numerical Identification of Elasticity Coefficients for Bending Problem. *Autex Research Journal* 2004; 4(4): 204-208.
6. Szablewski P. Analysis of the Stability of a Flat Textile Structure. *Autex Research Journal* 2006; 6(4): 204-215.
7. Bickley WG. The heavy elastic. *Philosophical Magazine and Journal of Science* 1934; Series 7, 17(113): 603-622.
8. Levien R. *The elastica: a mathematical history* (Report No. UCB/EECS-2008-103). University of California: Berkeley, 2008.
9. Szablewski P, Kobza W. Numerical Analysis of Peirce's Cantilever Test for the Bending Rigidity of Textiles. *Fibres and Textiles in Eastern Europe* 2003; 11(4): 54-57.
10. Huddleston JV. Effect of axial strain on buckling and post buckling behavior of elastic columns. *Developments in Theoretical and Applied Mechanics* 1970; 8: 263-273.
11. Nicolau MA, Huddleston JV. Compressible elastica on an elastic foundation. *Journal of Applied Mechanics* 1982; 49: 577-583.
12. Theocaris PS, Pannayotounakos DE. Exact solution of the nonlinear differential equation concerning elastic line of a straight rod due to terminal loading. *International Journal of Non-Linear Mechanics* 1982; 17: 395-402.
13. Theocaris PS, Pannayotounakos DE. Nonlinear elastic analysis of thin rods subjected to bending with arbitrary kinetic conditions of their cross-sections. *International Journal of Non-Linear Mechanics* 1982; 17: 119-128.
14. Holden JT. On the deflection of thin beams. *International Journal of Solids and Structures* 1972; 8: 1051-1055.
15. Skelton J. The effect of planar crimp in the measurement of mechanical properties of fibers, filaments, and yarns. *The Journal of The Textile Institute* 1967; 58: 533-556.
16. Frank F. Some loadextension properties of crimped fibers. *The Journal of The Textile Institute* 1960; 51: T83-T90.
17. Lanir Y. Constitutive equations for fibrous connective tissues. *Journal of Biomechanics* 1983; 16: 112.
18. Ling SC, Chow CH. The mechanics of corrugated collagen fibrils in arteries. *Journal of Biomechanics* 1977; 10: 71-77.
19. Kastelic J, Palley I, Baer E. A structural mechanical model of tendon crimping. *Journal of Biomechanics* 1980; 13: 887-893.
20. Korycki R, Więzowska A. Modelling of the temperature field within knitted fur fabrics. *Fibres and Textiles in Eastern Europe* 2011; 19, 1(84): 55-59.
21. Korycki R. Modeling of transient heat transfer within bounded seams. *Fibres and Textiles in Eastern Europe* 2011; 19, 5(88): 112-116.
22. Korycki R, Szafrńska H. Modelling of temperature field within textile in layers of clothing laminates. *Fibres and Textiles in Eastern Europe* 2013; 21, 4(100): 118-122.
23. Korycki R, Szafrńska H. Optimisation of pad thicknesses in ironing machines during coupled heat and mass transport. *Fibres and Textiles in Eastern Europe* 2016; 24, 1(115): 120-135.
24. Struik DJ. *Differential Geometry*. Addison-Wesley Publishing Company Inc.: Cambridge, 1950.

Received 07.03.2016 Reviewed 05.07.2016